

Antifibromyalgic Activity of Phytomolecule Niranthin: *In-Vivo* Analysis, Molecular Docking, Dynamics and DFT

Atul R. Chopade*, Vikram H. Potdar*, Suraj N. Mali^{†,‡,||}, Susmita Yadav[‡], Anima Pandey[§], Chin-Hung Lai[¶], Essa M. Saied^{||,*,**}, Oberdan Oliveira Ferreira⁺, Mozaniel Santana de Oliveira^{†,‡,++}, Shailesh S. Gurav^{§,§,¶} and Eloisa Helena de Aguiar Andrade^{†,‡,++}

*Department of Pharmacology, Rajarambapu College of Pharmacy, Kasegaon, Walwa, Sangli, Maharashtra 415404, India

⁺Postgraduate Program in Biotechnology and Biodiversity — BIONORTE Network, R. Augusto Corrêa, 01 — Guamá, Belém — PA, 66075-110, Brazil

[‡]Department of Pharmaceutical Sciences and Technology, Birla Institute of Technology, Mesra 835215, India

[§]Department of Pharmaceutical Sciences and Technology, Birla Institute of Technology, Mesra 835215, Jharkhand, India

[¶]Department of Medical Applied Chemistry, Chung Shan Medical University, Taichung 40241, Taiwan, ROC

^{||}Chemistry Department, Faculty of Science, Suez Canal University, Ismailia 41522, Egypt

^{**}Institute for Chemistry, Humboldt Universität zu Berlin, Brook-Taylor-Str. 2, 12489 Berlin, Germany

⁺⁺Adolpho Ducke Laboratory, Botany Coordination, Museu Paraense Emílio Goeldi, Belém, Pará, Brazil

^{††}Programa de Pós-Graduação em Ciências Biológicas — Botânica Tropical, Universidade Federal Rural da Amazônia, and Museu Paraense Emílio Goeldi, Av. Perimetral, 1901, Terra Firme, 66077-830, Belém, PA, Brazil

^{§§}Department of Chemistry, D. G. Ruparel College, Mumbai, Maharashtra, India

^{¶¶}Department of Chemistry, VIVA College, Virar, Maharashtra, India

^{|||}Corresponding author. E-mail: mali.suraj1695@gmail.com

ABSTRACT: Fibromyalgia (FM) is characterized by chronic pain and heightened sensitivity to painful stimuli. This study investigated the potential of Niranthin (NR), a natural compound derived from *Phyllanthus* species, in a rat model of FM. We employed a multifaceted approach to comprehensively assess the potential benefits of NR as a treatment for FM, including *in-vivo* analysis, molecular docking studies, and molecular dynamics (MD) simulations, and Density Functional Theory (DFT) calculations. Three doses of NR (5 mg/kg, 10 mg/kg and 20 mg/kg) significantly reduced mechanical allodynia induced by acidic saline injections. In an acute study, NR dosing increased the mechanical threshold in both ipsilateral and contralateral paws. In a four-day study, twice-daily NR treatment further elevated the mechanical threshold. Temporary treatment interruption led to a re-establishment of allodynia, but subsequent reinitiation of NR treatment remained effective, ruling out tolerance development. MD simulations were conducted to investigate the stability and dynamics of NR-target complexes, revealing stable binding interactions and conformational changes associated with NR binding. Docking calculations indicated that the NR molecule had a similar binding affinity to the drug Amiloride towards Acid-sensing ion channels (ASICs). NR showed interactions with amino acid residues, including LYS 373, ARG 370, GLU 374 and GLN 277. DFT calculations provided insights into the electronic and structural properties of NR and its interactions with FM-related molecular target ASICs. We propose that NR may modulate ASICs, leading to decreased pain sensitivity in FM rats. However, further research is required to fully understand the mechanism of action and explore NRs therapeutic potential for the treatment of FM.

KEYWORDS: Acid-sensing ion channels; *Phyllanthus*; Niranthin; pain; fibromyalgia; *in-silico*.

1. INTRODUCTION

Fibromyalgia (FM), a chronic pain disorder characterized by widespread musculoskeletal discomfort,

Received: 10 October 2023

Accepted: 24 November 2023

Published: 28 December 2023

fatigue, and cognitive disturbances, remains a challenging and enigmatic condition for both patients and healthcare professionals.¹ The multifactorial nature of FM, compounded by the lack of a clearly defined aetiology, has hindered the development of effective treatment options.² FM is identified by the presence of persistent widespread pain and sensitive points that indicate central nervous system (CNS) sensitization.⁴ Individuals with FM exhibit both qualitative and quantitative abnormalities in their experience of pain, resulting in allodynia and/or hyperalgesia.²

Several preclinical models have been developed to mimic various pain types, including acute, neuropathic, inflammatory, surgical and cancer-related pain encountered in clinical settings.³ However, the absence of suitable preclinical models has impeded basic drug discovery research in this area.² To address this issue, Sluka and colleagues⁴ introduced a rodent model involving acid saline-induced pain, which closely mimics musculoskeletal pain in humans. In this model, two injections of acidic saline (pH 4.0) into the gastrocnemius muscle, separated by 5 days, lead to a prolonged bilateral reduction in hind paw mechanical withdrawal responses.⁴ Nielsen and his team⁵ have pharmacologically characterized this model by assessing the effects of different analgesics. Notably, this model induces bilateral, widespread hyperalgesia affecting the paw, muscle and viscera, primarily mediated by central mechanisms.⁴ Acid-sensing ion channels (ASICs), a family of proton-gated ion channels, have emerged as potential players in the pathophysiology of chronic pain conditions.⁶ ASICs are expressed in various pain-sensing neurons and have been implicated in nociception and hyperalgesia.⁷ The link between ASICs and FM is an area of growing interest, as their dysregulation may contribute to the abnormal sensory processing and chronic pain experienced by FM patients.^{7–10}

Previously, we reported anti-FM activity of standardized extracts of *Phyllanthus amarus* and *Phyllanthus fraternus* in acidic saline-induced (ASI) chronic muscle pain model.² In our recent studies, we evaluated the anti-hyperalgesic activity of Niranthin (NR) [6-[(2R, 3R)-3-[(3,4-dimethoxyphenyl)methyl]-4-methoxy-2-(methoxymethyl) butyl]-4-methoxy-1,3-benzodioxole] Fig. 1, a product from *Phyllanthus* species, which was probably mediated by its analgesic and anti-inflammatory activities.^{11–13} However, the specific effects of NR on ASICs in the context of FM remained unexplored. Previously, we had also elucidated a possible positive modulation of the GABA-A/benzodiazepine

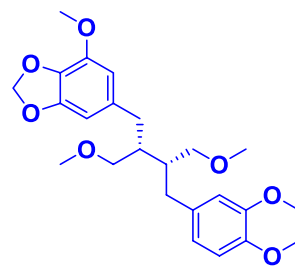


Fig. 1. (Color Online) The chemical structure of NR.

receptor complex by NR in relieving anxiety.¹⁴ Thus, considering the background literature² and our works on NR,^{11–14} we were encouraged to carry out the analysis of the specific testing of NR in acidic saline model. Moreover, as a plausible mechanism underlying, we did molecular docking of NR on ASIC receptor. The interconnecting role of ASIC and FM was supported by earlier literature.¹⁵ This research thus aims to explore the therapeutic potential of NR in the context of FM by employing a combination of *in-vivo* analysis, molecular docking studies, molecular dynamics (MD) simulations, and Density Functional Theory (DFT) calculations.^{17–26} By integrating these diverse techniques, we aim to provide a comprehensive assessment of NRs' capacity to alleviate FM symptoms while elucidating its underlying mechanisms of action.

2. RESULTS AND DISCUSSIONS

This study was undertaken to assess the effects of NR on mechanical allodynia² induced by repeated intramuscular injections of acidic saline.

2.1. Induction of chronic mechanical allodynia

From a total of 36 animals that received repeated injections of acidic saline, 31 rats (respondents) showed a significant reduction in paw withdrawal threshold in response to von Frey hair stimulation 24 h after the second injection. The remaining 13.888% ($n = 5$) of the nonrespondent animals displaying no responses to innocuous mechanical stimulation were excluded from the study. 24 h after the second injection, the mean mechanical withdrawal threshold of the experimental animals to mechanical stimuli of the ipsilateral paw decreased from 17.32 ± 0.152 g to 5.022 ± 0.604 g ($n = 30$). The details are summarized in Fig. 2. Out of the 31 respondents, 30 animals were selected for further studies.

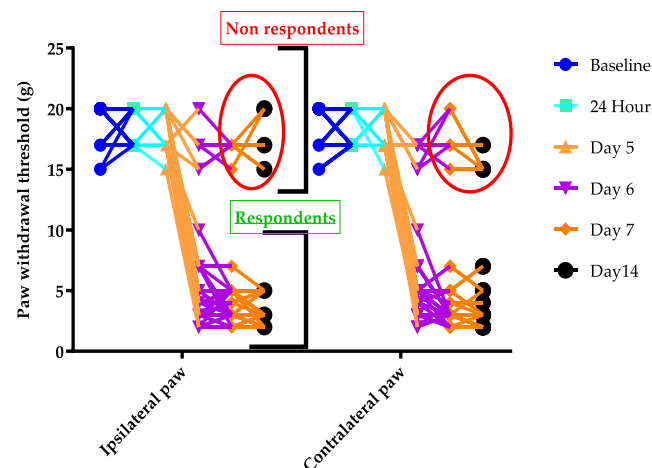


Fig. 2. (Color Online) Effect of repeated doses of acidic saline on mechanical paw withdrawal latency.

Figure 2 shows the effect of repeated injections of acidic saline in the gastrocnemius muscle of rats ($n = 36$). Withdrawal threshold (g) after stimulation of the plantar surface of the hindpaw was measured with von Frey hairs and the development of mechanical hyperalgesia was observed for both the ipsilateral and contralateral hindpaws. The various time points are baseline measured before the first injection, 24 h after the first injection, immediately before the second injection (on day -5) and on days 6, 7 and 14. Data are presented as mean \pm S.E.M. Number of responders was $n = 31$ and nonresponders $n = 5$, to mechanical stimuli after a day of first injection of acidic saline.

A similar reduction was shown by the contralateral paw from 18.361 ± 0.2677 g to 6.277 ± 0.728 g. This effect, until 3 weeks, significantly increased sensitivity remained for both paws after the second unilateral injection. The withdrawal threshold testing of the ipsilateral and contralateral paws showed no significant difference. Cold allodynia was tested for both the ipsilateral and contralateral paws by stimulating with acetone, but no changes were observed for either paw. From a total of 30 rats receiving two acidic saline repeated injections 83.33% ($n = 30$) had shown a significant reduction in paw withdrawal thresholds to mechanical stimulation by von Frey hairs, 24 h after the second acidic saline injection. The remaining 16.66% ($n = 6$) rats displayed reflex responses in exposure to innocuous mechanical stimuli similarly at the pre-injection stage and were excluded from this study. Responders' mean mechanical withdrawal threshold on the 14th day for ipsilateral paw was 2.865 ± 1.065 g

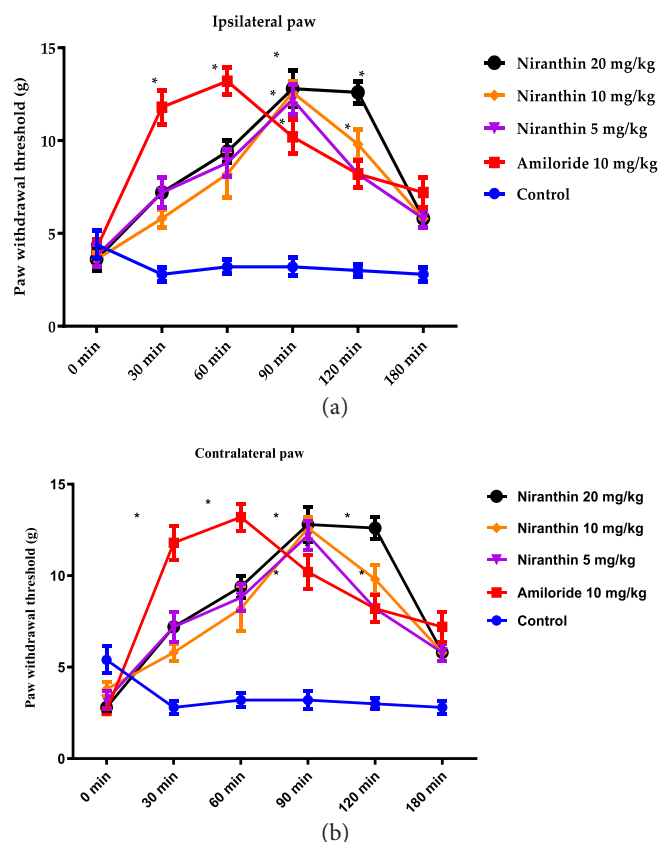


Fig. 3. (Color Online) Effect of NR on mechanical withdrawal threshold in acute responsive studies. NR induced an increase in ipsilateral (a) and contralateral (b) paw withdrawal threshold, which remained significantly different from baseline and vehicle-treated control for up to 180 min after injection of NR. Data are presented as mean \pm SEM, * $P < 0.05$ versus corresponding vehicle time points.

and nonresponders its 15.20 ± 0.92 g. The mean mechanical withdrawal threshold of responders in the contralateral paw was found to be 1.987 ± 0.078 g and for the nonresponders, it was 13.24 ± 0.2 g.

2.2. Modulation of mechanical allodynia by Niranthin

All studied NR doses (5 mg/kg, 10 mg/kg, and 20 mg/kg) showed significant mechanical allodynia reduction induced by acidic saline repeated injections. In the case of the acute study, ipsilateral paws' mechanical threshold was elevated to 13.97 ± 0.98 g, 13.11 ± 0.90 g and 11.98 ± 0.70 g for 5 mg/kg, 10 mg/kg and 20 mg/kg NR treatments, respectively (see Fig. 3(a)). While, for the contralateral paw, it was raised to 13.62 ± 0.84 g, 11.97 ± 0.70 g and 11.75 ± 0.5 g for 5 mg/kg, 10 mg/kg

and 20 mg/kg NR treatments, respectively (see Fig. 3(b)). After 90 min of their administration, a pronounced effect was observed, i.e., an increase in withdrawal threshold to mechanical stimuli for acute study. Twice a day administration of NR consequently for four days significantly reduced mechanical allodynia sensitivity of the ipsilateral paw, reaching to maximal of 15.80 ± 1.319 g, 16.20 ± 0.489 g and 16.40 ± 0.979 g for 5 mg/kg, 10 mg/kg and 20 mg/kg treatments, respectively (see Fig. 4(a)). The mechanical allodynia of the contralateral paw was elevated to 15.80 ± 1.805 g, 16.40 ± 0.979 g and 17.80 ± 0.969 g for 5 mg/kg, 10 mg/kg and 20 mg/kg treatments with NR, respectively (see Fig. 4(b)).

Treatment of NR was interrupted for two days (18th and 19th), and mechanical allodynia was re-established. NR treatment was then reinitiated again on the 20th day and it was noted that NR significantly reduces mechanical allodynia, excluding possibility of tolerance development.

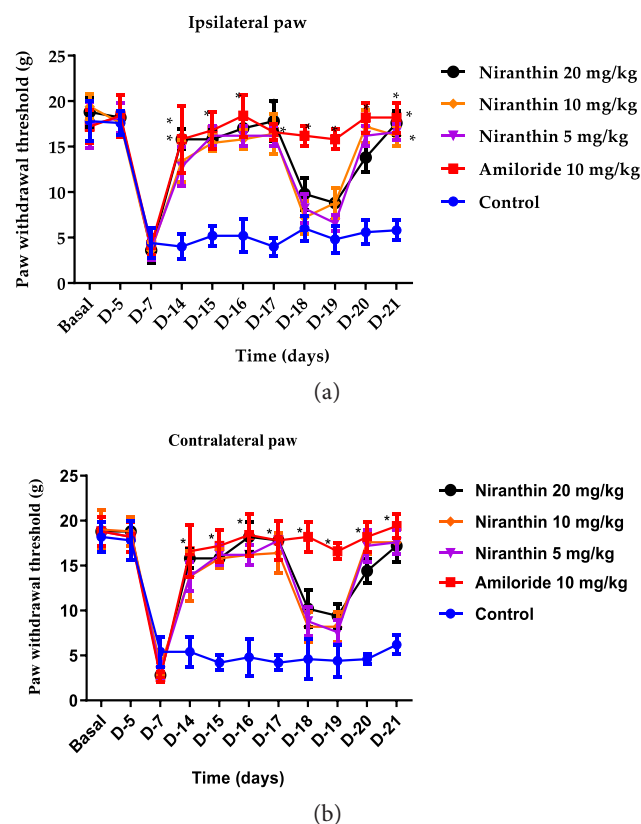


Fig. 4. (Color Online) Effect of NR on mechanical withdrawal threshold on chronic muscle allodynia. NR induced an increase in ipsilateral (a) and contralateral (b) paw withdrawal threshold, which remained significantly different from baseline and vehicle-treated control for up to 180 min after injection of NR. Data are presented as mean \pm SEM, * $P < 0.05$ versus corresponding vehicle time points.

Maximum possible effectiveness (MPE)

The details of the acute study are summarized in Fig. 5(a). It was observed that NR 20 mg/kg dose showed MPE of 255.66% for ipsilateral and 357.14% for contralateral paw. The NR 10 mg/kg dose shows MPE of 241.24% and 322.29% for ipsilateral and contralateral paws, respectively. While the MPE of NR 5 mg/kg treatment was 221.05% for the ipsilateral and 281.25% for the contralateral paw. The MPE of standard Amiloride treatment was 366.67% for the ipsilateral and 400.01% for the contralateral paw.

The details of the chronic study are summarized in Fig. 5(b). In the chronic study, it was seen that NR 20 mg/kg dose treated rats showed maximum possible effectiveness of 394.40% for ipsilateral and 550.01% for contralateral paws. The NR 10 mg/kg dose shows MPE of 326.30% and 456.25% for ipsilateral and contralateral paws, respectively. While, the NR 5 mg/kg treated rats showed MPE of 252.82% and 331.57% for ipsilateral and contralateral paws, respectively. The MPE of standard Amiloride treatment was 429.87% for the ipsilateral and 607.69% for the contralateral paw.

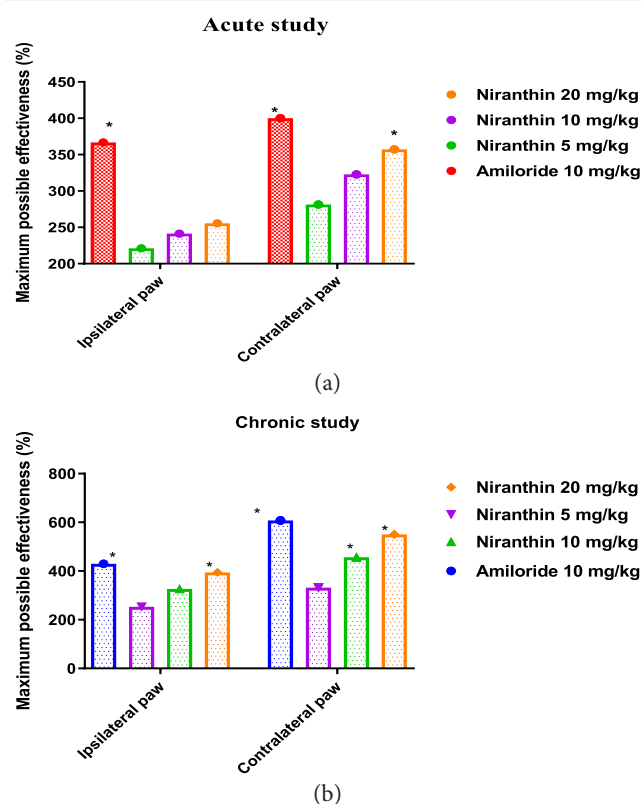


Fig. 5. (Color Online) Maximum possible effectiveness in percentage calculated for ipsilateral and contralateral paws for the (a) Acute study and (b) Chronic study. (the MPE values are represented only for the highest achieved values in a comparative manner; * $P < 0.05$ as compared to control).

Percentage inhibition of allodynia: In the case of the acute study the maximum percentage inhibition (MPI) of allodynia for 5 mg/kg, 10 mg/kg and 20 mg/kg dose treatment reached 53.43%, 55.82% and 57.01% inhibitions, respectively for ipsilateral paw. While, the MPI allodynia for 5 mg/kg, 10 mg/kg and 20 mg/kg dose-treated rats reach 56.619%, 59.105% and 60.348%, respectively, for the contralateral paw. The MPI of standard Amiloride treatment was 58.11% for the ipsilateral and 62.83% for the contralateral paw. The details of the acute study are summarized in Fig. 6(a).

In the case of chronic study, the MPI of allodynia for 5 mg/kg, 10 mg/kg and 20 mg/kg dose treatment reached 78.507%, 83.313% and 86.86%, respectively for ipsilateral paws. While the MPI allodynia for the contralateral paws for 5 mg/kg, 10 mg/kg and 20 mg/kg treated groups reached 82.72%, 91.423% and 93.909%, respectively. While the MPI of standard Amiloride treatment was 90.44% for the ipsilateral and 95.125% for the contralateral paw. The details of the chronic study are summarized in Fig. 6(b).

2.3. Results from docking

Based on the background literature¹⁶ supporting Amiloride-blockable ASICs, we conducted a theoretical analysis using molecular docking simulations. We performed molecular docking of the drug Amiloride against the target 'an ASIC in a resting state with calcium' (PDB ID: 5WKV) initially at pH. 7.4 (with default settings) followed by experimental conditions (*in-vivo*) with respect to the pH of acidic saline injection, i.e., at pH 4.0.¹⁷ Additionally, to identify a potential target for 'NR', we subjected it to docking as well. Docking results at pH. 7.4 indicated that molecule NR

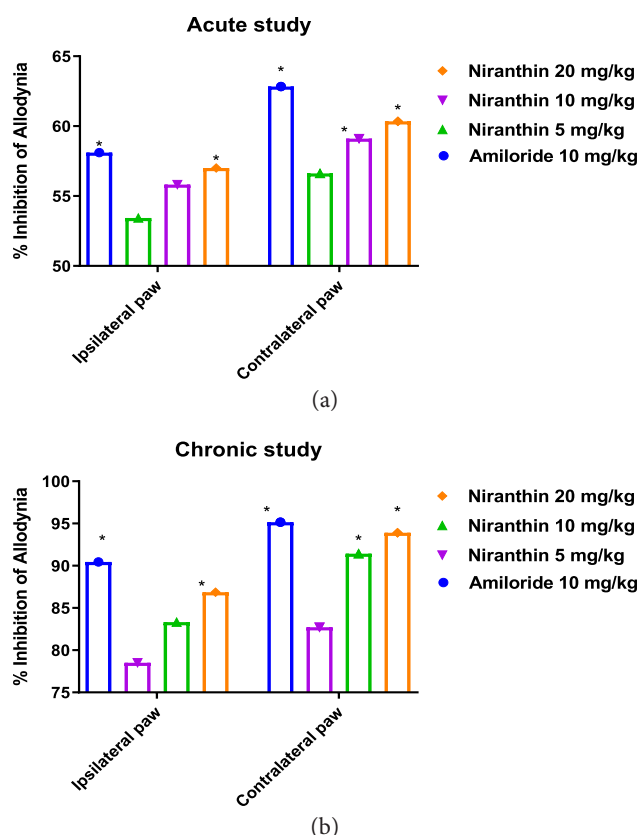


Fig. 6. (Color Online) Percentage inhibition of allodynia was calculated for ipsilateral and contralateral paws for the (a) Acute study and (b) Chronic study. (the values are represented only for the values where the highest percentage inhibition was observed comparatively; * $P < 0.05$ as compared to control).

(docking score: -93.23 Kcal/mol) exhibited a similar binding affinity to the drug Amiloride (docking score: -93.21 Kcal/mol). Standard Amiloride formed interactions with amino acid residues, such as GLN 135,

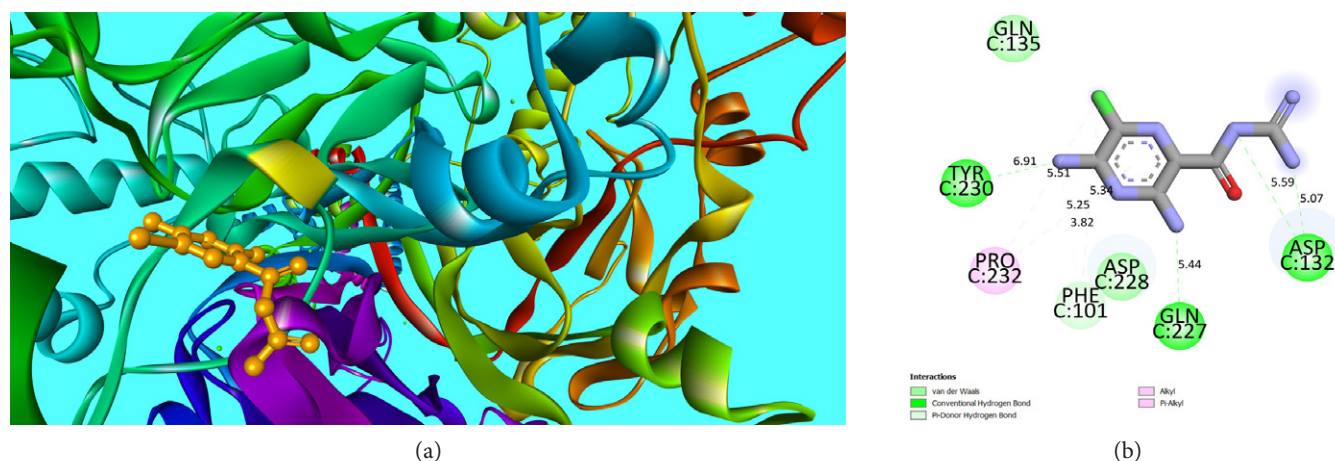


Fig. 7. (Color Online) A 2D-interaction diagram of Amiloride within the binding pocket of ASIC.

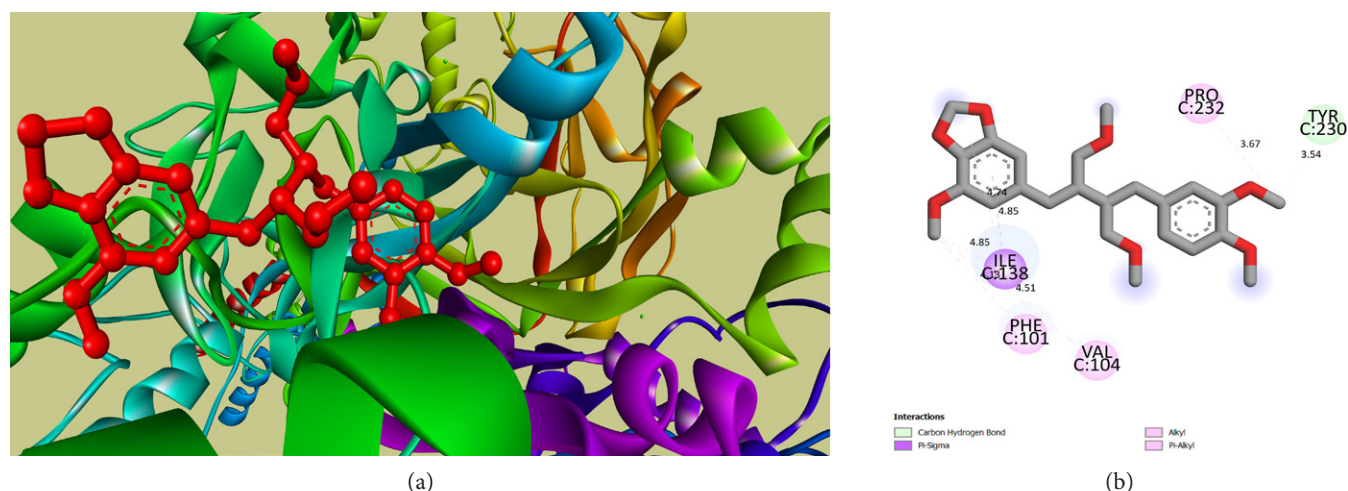


Fig. 8. (Color Online) A 2D-interaction diagram of NR within the binding pocket of ASIC.

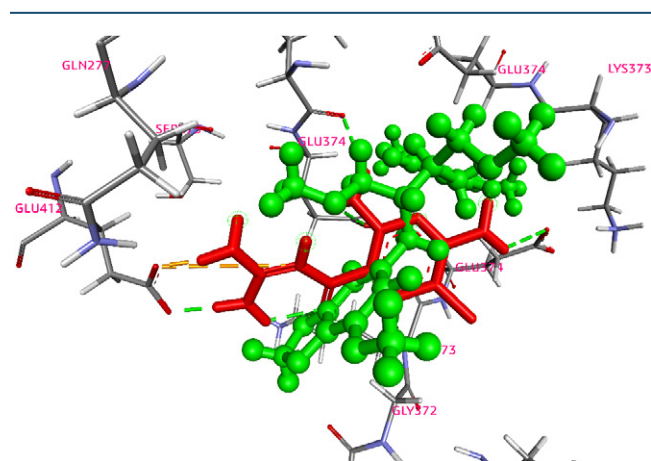


Fig. 9. (Color Online) 3D binding mode of NR (Green: Ball and Stick model) and Amiloride (Red) within the binding pocket of 5WKV.

TYR 230, PRO 232, ASP 228, GLN 227, GLU412 and ASP 132, through conventional H-bonding and alkyl, π -alkyl interactions (Fig. 7). Standard Amiloride however depicted interactions with amino acid residues, such as GLU 412, LYS 373, GLU 374 and GLN 277, through conventional H-bonding and charged interactions at pH 4.0. (refer to *Supplementary Information*). Similarly, NR displayed interactions with amino acid residues, including PRO 232, TYR 230, PHE 101, VAL 104 and ILE 138 (Fig. 8) at pH. 7.4. NR exhibited robust alkyl, π -alkyl interactions, or π -sigma interactions (Fig. 9). Based on the docking affinities, we conclude that NR shows a similar affinity towards ASICs as Amiloride, as demonstrated by *in-silico* studies.

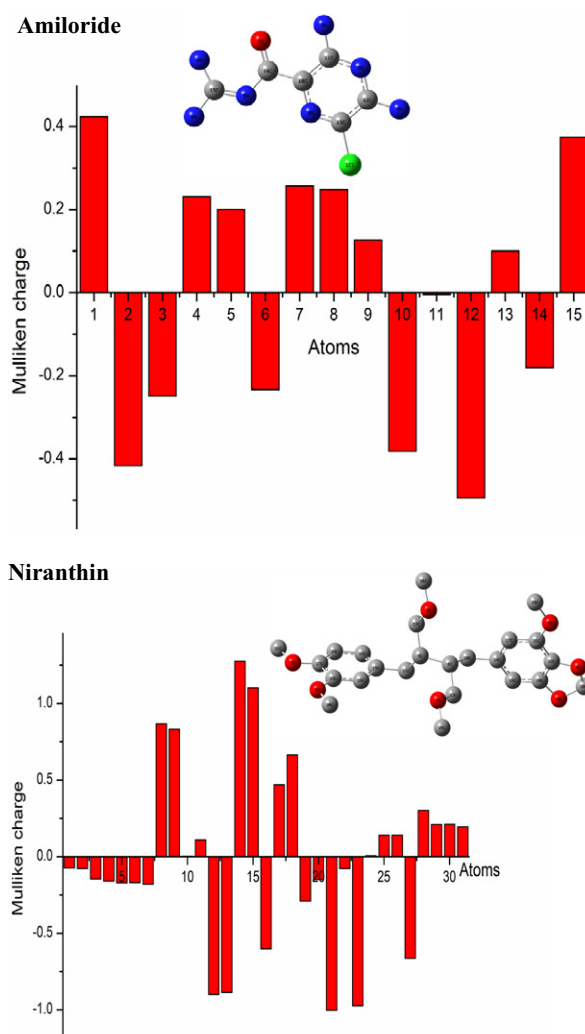


Fig. 10. (Color Online) The Mulliken charges of the studied compounds.

2.4. The mulliken charge analysis

The difference in the biological activities of the studied chemicals might correlate with the charge distributions within them.¹⁸ Therefore, the DFT-B3LYP method was adopted to calculate the Mulliken charges on the non-hydrogen atoms in the studied compounds. The calculated Mulliken charges of the two compounds are depicted in Fig. 10.

2.5. HOMO-LUMO analysis

Instead of thinking about the total electron density in a nucleophile, the electron density distribution in the highest occupied molecular orbital (HOMO) should be considered because electrons from this orbital have the most chance to participate in the nucleophilic attack, while the electron density distribution in the lowest unoccupied molecular orbital (LUMO) indicates whether a site is a good electrophilic site.¹⁹ The frontier molecular orbitals of the title compounds were further investigated in this study. As depicted in Fig. 11, the transition from the HOMO to LUMO orbital for Amiloride involves the mixing between the $\pi\pi^*$ transition and $n\pi^*$ transition whereas the transition from the HOMO to LUMO orbital for NR involves a charge transfer. Moreover, Amiloride has a smaller HOMO-LUMO gap (ΔE_g) than NR.

2.6. Molecular dynamics analysis

We carried out MD analysis for the complex 5WKV: NR for the period of 100 ns using the 'Desmond, Schrodinger, LLC, NY, 2023 module. In total 168,672 atoms were included throughout the simulation along with 49,485 water molecules. Standard NTP conditions were maintained. The Ligand Root Mean Square Deviation (RMSD) value (Fig. 12(a)) was retained below 4 Å; whereas RMSD values for C α backbone atoms, backbone atoms, and heavy atoms were retained below 4.2 Å. We also noticed that there were minimal amino acid residue fluctuations except residues at 400, 800 1200, etc. as indicated by The Root Mean Square Fluctuation (RMSF) graph (Fig. 12(b)). The Ligand-Root Mean Square Fluctuation (L-RMSF) value was observed below 5 Å (Fig. 13(a)). The protein-ligand contact plot indicated mainly water bridge interactions with amino acid residues such as Lys 422, Glu 426, Ala 428, Met 52, Ala 59, Leu 60, Thr 63, Asn 64, Arg 65, Gln 67 and Phe 70 (Figs. 13(b) and 13(c)). Amino acid residues Met 52, Leu 55, Ala56, Leu 58, Ala 59, Leu 60, Arg 65, Ile 66, Tyr 68, Phe 70 and Leu 71 represented hydrophobic interactions. Cys 62, Thr 63, Asn 64 and Gln 67 denoted mainly H-bonding interactions (Fig. 13(c)). The ligand torsions plot summarizes the conformational evolution of every rotatable bond (RB) in the ligand throughout the simulation trajectory (0.00 through 100.0s)

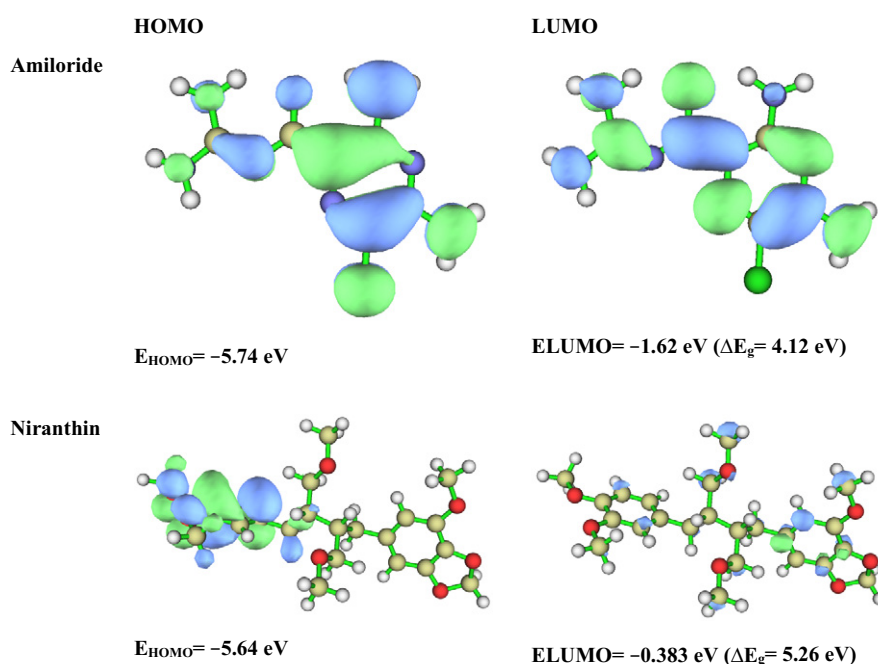


Fig. 11. (Color Online) The HOMO and LUMO of the studied compounds (the isovalue = 0.024 a.u.).

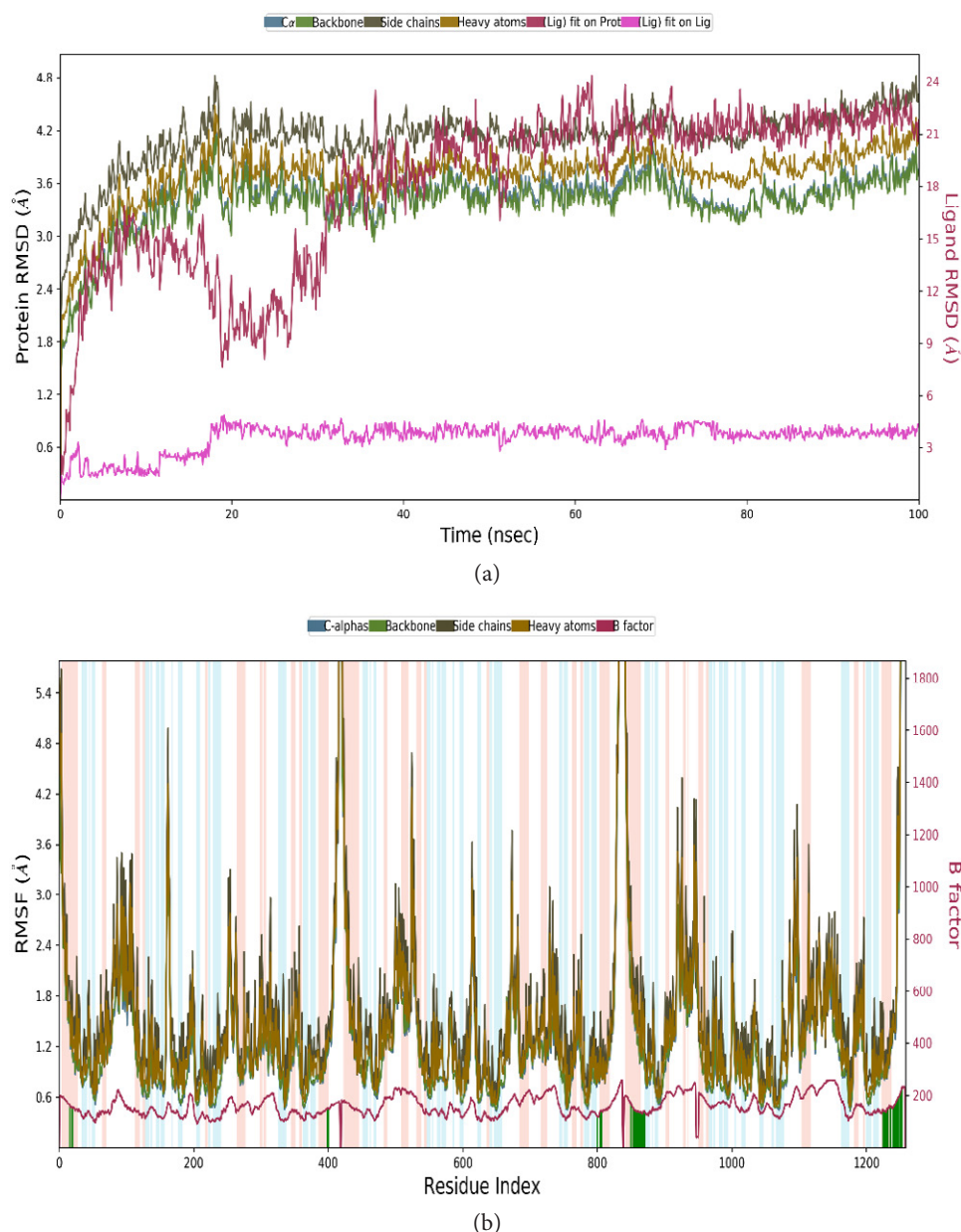


Fig. 12. (a) The RMSD and (b) RMSF plots for the complex 5WKV: NR for the period of 100 ns.

(Fig. 14). Figure 13(d) denotes ligand properties such as Ligand RMSD, Radius of Gyration (rGyr), Intramolecular Hydrogen Bonds (intra-HB), Molecular Surface Area (MolSA), Solvent Accessible Surface Area (SASA) and Polar Surface Area (PSA). Refer to Supplementary Information for detailed explanations.

2.7. Discussion

Anti-allodynia effects of Niranthin in acid saline-induced chronic allodynia

In this study, the administration of NR produced a dose-dependent reversal in mechanical hypersensitivity

in rats after repeated intra-muscular injection of acidic saline. Results indicated that the intraperitoneal administration of NR, twice a day, showed a significant antiallodynic effect in both paws. The acidic saline-induced chronic allodynia model is unique as it has very negligible muscle damage, and develops widespread hypersensitivity, mimicking the aspects of musculoskeletal pain associated with secondary allodynia spreading to paws.² Analgesics like morphine, diazepam, voltage-activated sodium channel blockers, glutamate receptor antagonists, potassium channel openers and others target a specified aspect of nociceptive transmission after systemic injection

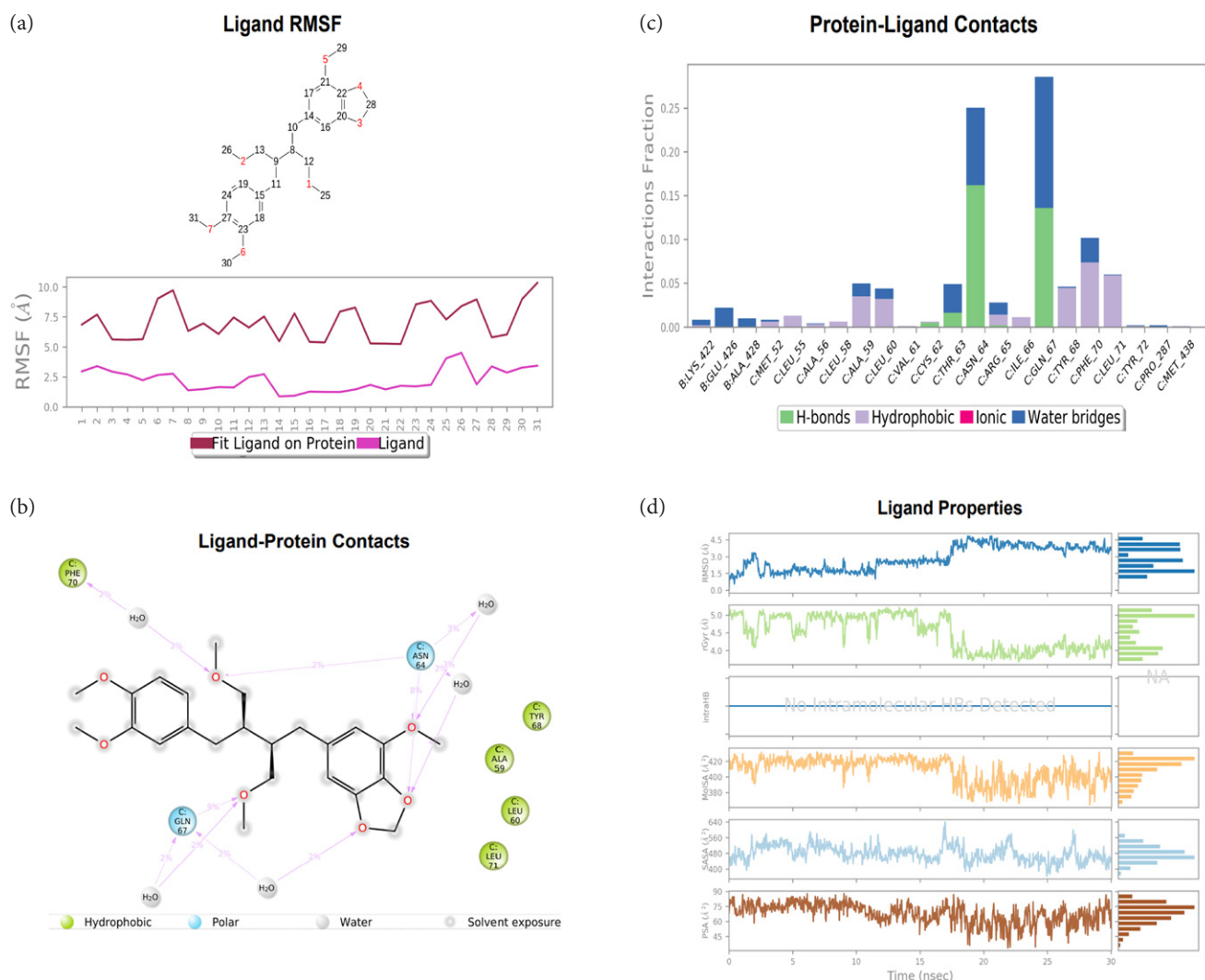


Fig. 13. (a) Ligand RMSF; (b) Ligand-Protein; (c) Protein-Ligand contacts and (d) Ligand properties.

which is very effective in the presently studied protocols.⁵ Earlier our studies demonstrated a possible positive modulation of the GABA-A/benzodiazepine receptor complex in relieving anxiety as we tested and recorded the effects of the NR using selective blocker as well as parallel *in-silico* analysis.¹⁴ NR has been shown to possess better analgesic potential in evaluated models of nociception being active centrally as well as peripherally. The findings of this study show the anti-allodynic action of NR that would probably be mediated via its ability to alter interact or modulate central sensitization.

Thus, highlighting NR potential interaction with ion channels could offer a novel approach to modulating pain signaling pathways. We performed a preliminary *in-silico* evaluation of NR interactions with basic

FM targets like Voltage-Activated Sodium Channel, glutamate receptors, potassium channels, but we did not find any positive clear findings for their involvement (Table 1). NR during *in-silico* docking studies revealed clear and unique interactions with ASICs, which led to further addition of molecular docking studies, molecular dynamic simulations, and DFT calculations supporting the *in-vivo* analysis. These complementary methods provide a comprehensive view of how NR interacts with ASICs and the potential consequences of this interaction at the molecular level. MD simulations helped to elucidate the dynamic behavior of the NR-ASIC complex, providing insights into stability and conformational changes, while DFT calculations offer information on the electronic structure and energetics of the complex.

Ligand Torsion Profile

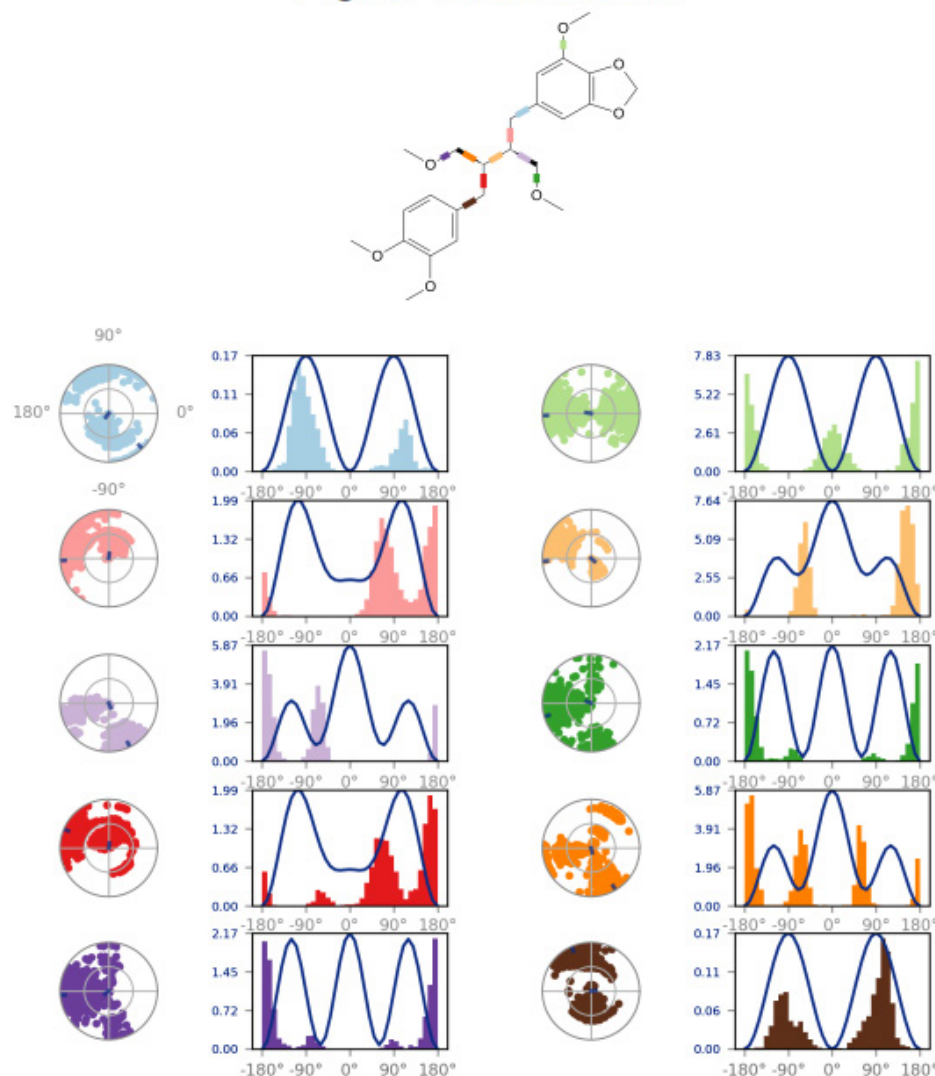


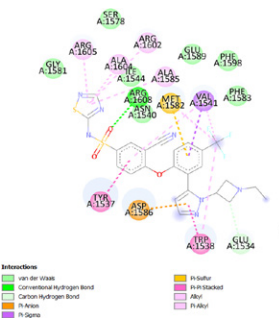
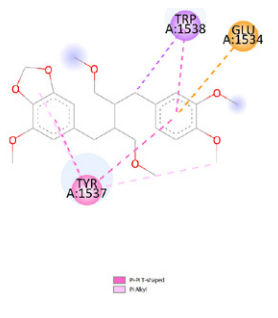
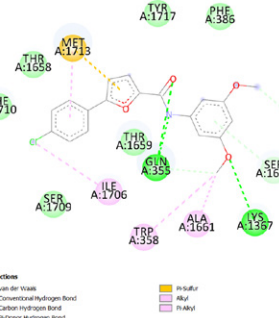
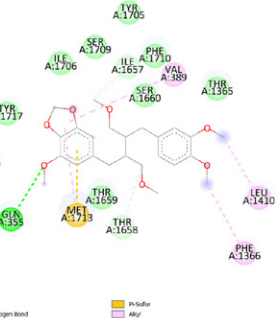
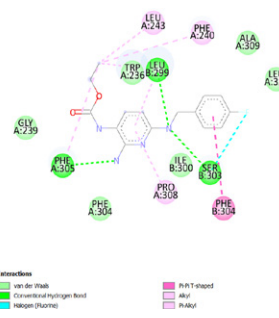
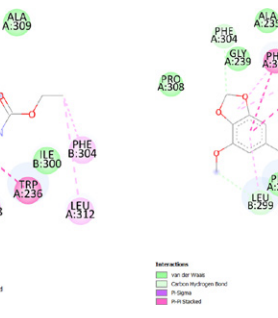

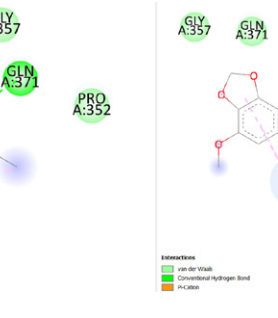
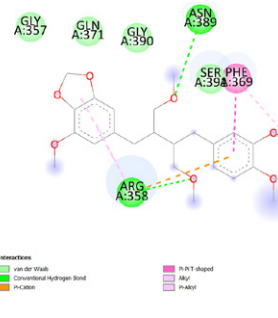
Fig. 14. Ligand torsion profile analysis.

Molecular docking analysis of Niranthin, and Target associated antagonists to check for off target involvement of NR

Current FM therapies include oral drugs targeting serotonin/noradrenaline (e.g., tricyclic antidepressants, serotonin/noradrenaline reuptake inhibitors), and voltage-gated calcium channel $\alpha 2$ delta subunit ligands like gabapentin/pregabalin.²⁷ Peripheral sensory generators suggest topical medicines. FM symptoms align with altered K^+ channel functioning seen in channelopathies. Persistent/neuropathic pain links to acquired/inherited K^+ channel alterations. K_v channels may underlie neuromyotonia. Some FM treatments alter K^+ channel activity.²⁷

Voltage-gated sodium channels (VGSCs/Navs) are crucial for cellular/molecular electrical signal transduction.²⁸ They initiate action potentials in excitable cells like neurons, myocytes, and neuroendocrine cells. Glial cells around nerve fiber nuclei have transporters, glutamate receptors, and major histocompatibility complex molecules.²⁸ Dorsal root ganglia neurons express nociceptive ion channels (Nav1.7, Nav1.8, Nav1.9, calcium channels, transient receptor potential channels). Nav1.7 and Nav1.8 play a role in inflammatory/neuropathic pain.²⁸ N-methyl-d-aspartate receptor (NMDAR) activation increases spinal cord/brain pathway sensitivity, particularly in pain processing. NMDAR activity is elevated in FM, making it a therapeutic target.²⁹

Table 1. Docking Screening of NR and associated co-crystallized ligands or antagonists against various off targets involved in FM (2D interaction diagrams against various targets have shown in the table).

Other Target's	Ligands Targeted/Antagonists/Co-crystal Ligands	
voltage-gated sodium channel 1.7 (Nav1.7) (pdb id: 5ek0)	Co-crystallized Ligand, 5P2 (Docking Score: – 77.23 Kcal/mol)	Niranthin (Docking Score: – 70.98 Kcal/mol)
		
voltage-gated sodium channel 1.8 (Nav1.8) (pdb id: 7we4)	Co-crystallized Ligand, 95T (Docking Score: – 112.56 Kcal/mol)	Niranthin (Docking Score: – 95.67 Kcal/mol)
		
The Kv7 (also referred to as KCNQ) potassium channel (pdb id: 7cr2)	Flupirtine (Docking Score: – 125.23 Kcal/mol)	Retigabine (Docking Score: – 130.53 Kcal/mol)
		
N-Methyl-D-Aspartate (NMDA) receptor (pdb id: 3qe1)	Ifenprodil (Docking Score: – 80.72 Kcal/mol)	Flupirtine (Docking Score: – 79.32 Kcal/mol)
		
		Niranthin (Docking Score: – 70.98 Kcal/mol)
		

Thus, considering facts, we carried out a docking analysis of NR, target-associated antagonists or co-crystallized ligands to exclude the possibility of NR acting on off-targets involved in FM.^{30–33} As we see from Table 1 results, it is very clear that NR has lesser interactions (lesser docking scores) *in-silico* towards targets other than ASICs, which prompted us to check the further *in-vivo* study associated with ASIC. This preliminary analysis depicts the fact that NR may act selectively on ASICs.

Plausible role of Niranthin role in modulating acid-sensing ion channels: evidence from Molecular docking, Dynamics and DFT studies

FM is a complex chronic pain syndrome characterized by widespread musculoskeletal pain, fatigue, sleep disturbances and cognitive impairment.¹ While its exact etiology remains unclear, emerging evidence suggests the involvement of ASICs in the development and maintenance of pain in FM.¹⁵ ASICs are a family of proton-gated cation channels expressed in sensory neurons and play a key role in nociceptive signal transduction.¹⁵ Acidosis in the tissues, which can occur in response to inflammation or metabolic changes, can activate ASICs, leading to neuronal excitation and pain hypersensitivity.²⁰ In FM, there is evidence of increased tissue acidosis and aberrant sensory neuron activity, making ASICs a relevant target for investigation.²⁰ The NRs investigation for modulation of ASICs is grounded in the idea that by interfering with ASIC activation, it may mitigate the pain signals associated with FM. *In vitro* studies and molecular docking simulations have provided initial evidence supporting the binding of NR to ASICs, suggesting its potential as an ASIC modulator.

Modulating ASICs offers a promising approach to FM treatment. By inhibiting ASICs, NR may reduce neuronal hyperexcitability and pain sensitivity, which are hallmark symptoms of the condition. This approach aligns with the growing understanding that FM is not solely a disorder of central sensitization but involves peripheral sensitization as well. Targeting ASICs may address this peripheral component and alleviate pain at its source.

The *in-vivo* analysis conducted in this study is a crucial component, as it bridges the gap between the theoretical knowledge of NRs interaction with ASICs and its actual effects in animals. Molecular docking, dynamics simulations, and DFT calculations represent the foundational pillars of this research, as they offer a theoretical framework to understand the interaction between NR and ASICs at the molecular level. The

molecular docking studies elucidate the binding affinity and binding modes of NR with ASICs, indicating the likelihood of an effective interaction. Additionally, the dynamics simulations provide insights into the conformational changes and stability of the NR-ASIC complex, which are essential for predicting the long-term effects of this interaction. DFT calculations offer information regarding the electronic structure, charge distribution, and energy profiles of the complex, providing a more detailed understanding of the molecular interaction.

One of the major strengths of this study is the integration of both *in-vivo* and *in-silico* approaches. The combined evidence from these diverse methodologies adds credibility to the findings. The research findings point towards the modulation of ASICs as a potential mechanism of action for NR. However, the precise molecular mechanisms underlying this modulation remain to be fully elucidated. Future research should focus on uncovering the signaling pathways and cellular responses triggered by NR-ASIC interaction. However, further research, particularly in the form of clinical trials, is required to confirm the safety and efficacy of NR for FM patients. If successful, this research could potentially lead to the development of a novel and more effective therapeutic approach for individuals suffering from this challenging condition.

3. MATERIALS AND METHODS

3.1. Chemicals

The pure Phytomolecule, NR [6-[(2R,3R)-3-[(3,4-dimethoxyphenyl) methyl]-4-methoxy-2-(methoxymethyl)butyl]-4-methoxy- 1,3-benzodioxole] (Product code: N006, Lot. no.: T18C277) was purchased from Natural Remedies Pvt. Ltd., Bangalore, India. NR purity was certified with the help of HPLC analysis above 95.0%. Dimethyl sulphoxide (DMSO) and sodium chloride (NaCl) were purchased from Loba Chemicals.

3.2. Animals

Adult Wistar female rats weighing (range: 250–350 gms; aged between 9 and 11 weeks) were used in this study. The standard environmental conditions as per ethical norms were maintained. Standard diet and water *ad libitum* were available for the entire experimental protocol. Approved protocol number [RCP/18-19/P-20A] was taken from by institutional animal ethical committee (IAEC) constituted for control and supervision of

experimental animals by the Ministry of Environmental and Forests, Government of India, New Delhi.

3.3. Experimental details

3.3.1. Chronic muscular allodynia induction

The previously described method of induction of chronic muscle-mediated pain was used.^{18–20} The lateral left gastrocnemius muscle was injected with 100 ml of hydrochloric acid in saline solution (9 g NaCl/liter; pH adjusted to 4.0 ± 0.1). After five days the same left lateral gastrocnemius muscle was re-injected with the same protocol. Out of the 36 animals (31 respondents), 30 animals were selected for further studies while the other nonrespondents were excluded from the study.

3.3.2. Experimental design

The responders' rats ($n = 30$) were divided into five groups of six animals each as follows:

- **Group A** served as the control group (hyperalgesic rats) injected with vehicle DMSO 0.2 ml intraperitoneally.
- **Group B** served for standard drug comparison injected intraperitoneally with an Amiloride inhibitor for ASICs at a dose of 10 mg/kg. Previous reports support that Amiloride shows antinociceptive effects in animals and humans through the inhibition of ASICs.
- **Group C** served as for test drug injected intraperitoneally with NR 5 mg/kg.
- **Group D** served as for test drug injected intraperitoneally with NR 10 mg/kg.
- **Group E** served as for test drug injected intraperitoneally with NR 20 mg/kg.

Chronic muscular allodynia was induced by injecting acidic saline (pH 4.0) into the gastrocnemius muscle for 14 consecutive days; in all five groups of rats. Acute responses were evaluated around 48 hours after the second acidic saline injection of rats injected with NR (5 mg/kg, 10 mg/kg and 20 mg/kg, i.p.) or vehicle alone. The mechanical allodynic activity of NR was evaluated at set time points. Investigation of chronic treatment of mechanical allodynia, NR twice a day was administered (apart intervals of 12 h) to the grouped rats for a week. For two days, the treatment was interrupted such as on the 18th and 19th day but was restarted again on the 20th day for investigation tolerance development.

The allodynia response evaluation being of nociceptive type was performed 90 min after the first daily administration (the time point was noted where the maximal inhibition was maximum in the acute study).

3.3.3. Mechanical allodynia behavioral testing

Rats were placed on an elevated metal mesh grid to test mechanical allodynia by stimulating the paw plantar surface. The series of von Frey nylon hairs or filament (2–20 g) was used to assess mechanical allodynia, filament was applied with increasing force until the rat withdrew its paw. Each hair was applied two times and the threshold in grams was noted as the lowest force that caused withdrawal stimuli. Prior calibrated Von Frey nylon was used during the entire course of the study which ensured consistency of applied forces. Rats testing mechanical withdrawal stimuli were done prior to the first acidic saline injection, before the second injection and subsequently further on day 5, 24 h after the second injection, on day 7 for the acute study and subsequently later on from the 14th day to the 21st day after the acidic saline second injection.

3.3.4. Measurement of maximum possible effectiveness [%] and inhibition of allodynia [%]

The % maximum possible effectiveness and % inhibition of allodynia were calculated using Eqs. (A) and (B) and the calculated arithmetic means in instances for detecting the main effects for acute and chronic studies.

(a) Maximum possible effectiveness in percentage (%)

Maximum possible effectiveness (%) = $\frac{\text{post NR treatment latency} - \text{post repeated acidic saline treatment latency}}{\text{post NR treatment latency}} \times 100$ (Eq. (A)).

For this study in the acute study, the post latency was recorded 48 h after the second injection and for the chronic study, latency was recorded 2 weeks after the first injection.

(b) Inhibitory Percentage of allodynia

Inhibitory Percentage of allodynia (%) = $\frac{\text{test latency} - \text{mean basal withdrawal latency}}{\text{mean basal withdrawal latency}} \times 100$ (Eq. (B)).

In Eq. (B), the mean of the basal mechanical withdrawal threshold is calculated ipsilaterally plus contralaterally for both paws and only in responders

($n = 30$), and the value is estimated at 3.147 ± 1.074 for ipsilateral paw and 3.186 ± 0.1356 for contralateral paw, to calculate % effects produced by the after intraperitoneal NR administration.

3.4. Statistical analysis

GraphPad Prism software version 6.01[®], 1992–2012 was used for statistical calculation of obtained data. Data for mechanical allodynia are represented as mean \pm SEM. One-way repeated ANOVA (analysis of variance) was used to analyze the effects of NR, following Tukey's test posthoc testing. $P < 0.05$ was considered to be statistically significant in all cases.

3.5. Molecular docking analysis and molecular dynamics

We conducted the molecular docking analysis using the software 'Glide, Schrodinger, LLC, NY, 2023'. First, The 2D structures for NR and Amiloride were obtained from the PubChem database (<https://pubchem.ncbi.nlm.nih.gov/compound/Niranthin> and <https://pubchem.ncbi.nlm.nih.gov/compound/Amiloride>, respectively). Subsequently, all these 2D structures were converted and optimized into 3D forms using the Maestro workflow and with the 'LigPrep' module, 2023. As for the 3D crystal structure of ASIC (PDB ID: 5WKV), we retrieved it from the Protein Data Bank (<https://www.rcsb.org/structure/5wkV>). While preparing ligands, we kept pH equivalent to acidic saline injection (i.e., 4.0). The protein was prepared as per the default settings of 'Protein Preparation Wizard'. The grid parameters were set to X: -13.65 , Y: 1.6 , and Z: -0.13 \AA . Finally, we executed the docking calculations using 'XP settings'. For docking validation, we did re-docking of co-crystallized ligand, 2-acetamido-2-deoxy-beta-D-glucopyranose against the binding site of 5WKV. The RMSD was retained as $\text{RMSD} = 0.32 \text{ \AA}$ (refer to *Supplementary Information*). The molecular docking protocols for other targets with pdb codes: 5ek0, 7we4, 7cr2 and 3qel were followed from earlier publications.^{30–33} The common methodologies for docking were carried out from our earlier reports.^{34–38} For this study, MD analysis was performed using 'the Desmond' module using the default settings for 100 ns. For this, we referred to our earlier publication for setting up the MD system. The protein structure with ligand, NR was enclosed within orthorhombic boxes measuring $125 \text{ \AA} \times 125 \text{ \AA} \times 125 \text{ \AA}$. These structures were then immersed in water molecules modeled using

the single point charge (SPC) model, a part of the Desmond System Builder software developed by Schrödinger, LLC, based in New York, NY, USA, 2023. To ensure overall system neutrality, counter ions were added, and a constant salt concentration of 0.15 M NaCl was maintained throughout the simulations. The simulations were conducted in triplicate for a duration of 100 ns using the Desmond software, with distinct initial velocity assignments for each atom in each replicate. The OPLS forcefield was employed to describe the molecular interactions within the systems. Prior to the main production simulation run, all simulation systems underwent Desmond's default eight-stage relaxation protocol. To control system parameters during the simulations, the isotropic Martyna–Tobias–Klein barostat was utilized to maintain the pressure at 1 atmosphere, while the Nose–Hoover thermostat was employed to keep the temperature constant at 300 Kelvin.

3.6. Theoretical analysis

The gas-phase structures of the tested compounds were optimized using DFT in conjunction with the basis set 6-311++G**,^{21–25} The DFT calculation was performed by the hybrid B3LYP method, which is based on the idea of Becke and considers a mixture of the exact (HF) and DFT exchange utilizing the B3 functional, together with the LYP correlation functional. After obtaining the converged geometry, the harmonic vibrational frequencies were calculated at the same theoretical level to confirm the number of imaginary frequencies is zero for the stationary point. Both the geometry optimizations and harmonic vibrational frequency analyses of the studied compounds were done by the Gaussian 09 program.²⁶ Moreover, the quantum chemical descriptors derived from the conceptual DFT were calculated for the respective molecule.

4. CONCLUSIONS

The results of this study of the muscle-mediated pain model suggest that allodynia can be alleviated by NR probably by interacting with ASICs or other probable different unexplored mechanisms. But our computational data support the facts that ASIC3 modulation by NR might probably help in the significant reduction of allodynia in rats. Based on the combined *in-vivo* and *in-silico* studies we suggest that NR may hold promise as a potential therapeutic agent to treat FM. NR's ability to modulate ASIC-3 channels could lead to pain relief and improved quality of life in FM rats. However,

further research would be necessary for higher *in-vivo* models to fully understand the mechanisms involved and to determine the efficacy, safety, and potential side effects of NR in human FM patients.

Supplementary. Figure S1. Re-docking of co-crystallized ligand 2-acetamido-2-deoxy-beta-D-glucopyranose within the same binding site of 5WKV. RMSD = 0.32 Å; Figure S2: docking of co-crystallized ligand 2-acetamido-2-deoxy-beta-D-glucopyranose within the same binding site of 5WKV.

DATA AVAILABILITY

Data will be made available upon reasonable request from authors.

AUTHOR CONTRIBUTIONS

All authors contributed equally.

CONFLICT OF INTEREST

The authors declared no conflict of interests.

FUNDING INFORMATION


There is no funding information for this paper.

SUPPLEMENTARY INFORMATION

The Supplementary Information are available at: <https://www.worldscientific.com/doi/suppl/10.1142/S2737416523500655>.

ORCID

Suraj N. Mali  <https://orcid.org/0000-0003-1995-136X>

Mozaniel Santana de Oliveira  <https://orcid.org/0000-0002-4076-2443>

References

1. Clauw, D. J. Fibromyalgia: An overview. *Amer. J. Med.* **2009**, 122 (12), S3–S13.
2. Chopade, A. R.; Sayyad, F. J. Antifibromyalgic activity of standardized extracts of *Phyllanthus amarus* and *Phyllanthus fraternus* in acidic saline induced chronic muscle pain. *Biomed. Aging Pathol.* **2014**, 4 (2), 123–130.
3. Sandkuhler, J. Models and mechanisms of hyperalgesia and allodynia. *Physiol. Rev.* **2009**, 89 (2), 707–758.
4. Sluka, K. A.; Kalra, A.; Moore, S. A. Unilateral intramuscular injections of acidic saline produce a bilateral, long-lasting hyperalgesia. *Muscle Nerve: Official J. Amer. Assoc. Electrodiagnostic Med.* **2001**, 24 (1), 37–46.
5. Nielsen, A. N.; Mathiesen, C.; Blackburn-Munro, G. Pharmacological characterisation of acid-induced muscle allodynia in rats. *Euro. J. Pharmacol.* **2004**, 487 (1–3), 93–103.
6. Wemmie, J. A.; Taugher, R. J.; Kreple, C. J. Acid-sensing ion channels in pain and disease. *Nature Rev. Neurosci.* **2013**, 14 (7), 461–471.
7. Hung, C. H.; Lee, C. H.; Tsai, M. H.; Chen, C. H.; Lin, H. F.; Hsu, C. Y.; Lai, C. L.; Chen, C. C. Activation of acid-sensing ion channel 3 by lysophosphatidylcholine 16: 0 mediates psychological stress-induced fibromyalgia-like pain. *Ann. Rheum. Dis.* **2020**, 79 (12), 1644–1656.
8. Sluka, K. A.; Winter, O. C.; Wemmie, J. A. Acid-sensing ion channels: A new target for pain and CNS diseases. *Current Opin. Drug Discov. Develop.* **2009**, 12 (5), 693.
9. Lin, J. H.; Hung, C. H.; Han, D. S.; Chen, S. T.; Lee, C. H.; Sun, W. Z. and Chen, C. C. Sensing acidosis: Nociception or snception?. *J. Biomed. Sci.* **2018**, 25 (1), 1–8.
10. Heusser, S. A.; Pless, S. A.; Acid-sensing ion channels as potential therapeutic targets. *Trends Pharmacol. Sci.* **2021**, 42 (12), 1035–1050.
11. Chopade, A. R.; Salunkhe, V. R.; Patil, P. A.; Burade, M. R.; Somade, P. M.; Mali, S. N.; Pandey, A. Antinociceptive investigations of niranthin in complete Freund's adjuvant-induced chronic pain in mice. *Recent Adv. Inflam. Allergy Drug Disc.* **2021**, 15 (2), 108–112.
12. Chopade, A. R.; Sayyad, F. J.; Pore, Y. V. Molecular docking studies of phytocompounds from the *phyllanthus* species as potential chronic pain modulators. *Sci. Pharmac.* **2015**, 83 (2), 243–267.
13. Chopade, A. R.; Sayyad, F. J. Pain modulation by lignans (phyllanthin and hypophyllanthin) and tannin (corilagin) rich extracts of *Phyllanthus amarus* in carrageenan-induced thermal and mechanical chronic muscle hyperalgesia. *Phytoth. Res.* **2015**, 29 (8), 1202–1210.
14. Chopade, A. R.; Somade, P. M.; Somade, P. P.; Mali, S. N. Identification of anxiolytic potential of niranthin: In-vivo and computational investigations. *Nat. Products Bioprospect.* **2021**, 11, 223–233.
15. Yen, L. T.; Hsieh, C. L.; Hsu, H. C.; Lin, Y. W. Targeting ASIC3 for relieving mice fibromyalgia pain: Roles of electroacupuncture, opioid, and adenosine. *Sci. Rep.* **2017**, 7 (1), 46663.
16. Ugawa, S.; Ueda, T.; Ishida, Y.; Nishigaki, M.; Shibata, Y.; Shimada, S. Amiloride-blockable acid-sensing ion channels are leading acid sensors expressed in human nociceptors. *J. Clin. Invest.* **2002**, 110 (8), 1185–1190.

17. Yoder, N.; Yoshioka, C.; Gouaux, E. Gating mechanisms of acid-sensing ion channels. *Nature* **2018**, 555 (7696), 397–401.
18. Hansch, C.; Fujita, T. p - σ - π analysis. A method for the correlation of biological activity and chemical structure. *J. Amer. Chem. Soc.* **1964**, 86 (8), 1616–1626.
19. Mali, S. N.; Anand, A.; Zaki, M. E.; Al-Hussain, S. A.; Jawarkar, R. D.; Pandey, A.; Kuznetsov, A. Theoretical and anti-Klebsiella pneumoniae evaluations of substituted 2, 7-dimethylimidazo [1, 2-a] pyridine-3-carboxamide and Imidazopyridine hydrazide derivatives. *Molecules* **2023**, 28 (6), 2801.
20. Wang, Y. Z.; Xu, T. L. Acidosis, acid-sensing ion channels, and neuronal cell death. *Molecular Neurobio.* **2011**, 44, 350–358.
21. McLean A. D.; Chandler, G. S. Contracted Gaussinabasis sets for molecular calculations. 1. 2nd row atoms, $Z = 11$ –18. *J. Chem. Phys.* **1980**, 72, 5639–5648.
22. Raghavachari, K.; Binkley, J. S.; Seeger, R.; J. A. Pople, Self-consistent molecular orbital methods. 20. Basis set for correlated wave-functions. *J. Chem. Phys.* **1980**, 72, 650–654.
23. Becke, A. D. Density-functional thermochemistry. III. The role of exact exchange. *J. Chem. Phys.* **1993**, 98, 5648–5652.
24. Lee C.; Yang, W.; Parr, R. G. Development of the Colle–Salvetti correlation-energy formula into a functional of the electron density. *Phys. Rev. B* **1988**, 37, 785–789.
25. Miehlich, B.; Savin, A.; Stoll and H. Preuss, Results obtained with the correlation energy density functionals of becke and Lee, Yang and Parr. *Chem. Phys. Lett.* **1989**, 157, 200–206.
26. Frisch, M. J.; Trucks, G. W.; Schlegel, H. B.; Scuseria, G. E.; Robb, M. A.; Cheeseman, J. R.; Scalmani, G.; Barone, V.; Mennucci, B.; Petersson, G. A.; Nakatsuji, H.; Caricato, M.; Li, X.; Hratchian, H. P.; Izmaylov, A. F.; Bloino, J.; Zheng, G.; Sonnenberg, J. L.; Hada, M.; Ehara, M.; Toyota, K.; Fukuda, R.; Hasegawa, J.; Ishida, M.; Nakajima, T.; Honda, Y.; Kitao, O.; Nakai, H.; Vreven, T.; Montgomery, Jr., J. A.; Peralta, J. E.; Ogliaro, F.; Bearpark, M.; Heyd, J. J.; Brothers, E.; Kudin, K. N.; Staroverov, V. N.; Keith, T.; Kobayashi, R.; Normand, J.; Raghavachari, K.; Rendell, A.; Burant, J. C.; Iyengar, S. S.; Tomasi, J.; Cossi, M.; Rega, N.; Millam, J. M.; Klene, M.; Knox, J. E.; Cross, J. B.; Bakken, V.; Adamo, C.; Jaramillo, J.; Gomperts, R.; Stratmann, R. E.; Yazyev, O.; Austin, A. J.; Cammi, R.; Pomelli, C.; Ochterski, J. W.; Martin, R. L.; Morokuma, K.; Zakrzewski, V. G.; Voth, G. A.; Salvador, P.; Dannenberg, J. J.; Dapprich, S.; Daniels, A. D.; Farkas, O.; Foresman, J. B.; Ortiz, J. V.; Cioslowski, J.; Fox, D. J. Gaussian 09 Revision E.01, Gaussian, Inc., Wallingford CT, 2013.
27. Lawson, K. Kv7 channels a potential therapeutic target in fibromyalgia: A hypothesis. *World J. Pharmacol.* **2018**, 7 (1), 1–9.
28. Martínez-Lavín, M. Dorsal root ganglia: Fibromyalgia pain factory? *Clin Rheumatol.* **2021**, 40, 783–787, <https://doi.org/10.1007/s10067-020-05528-z>.
29. Littlejohn, G.; Guymer, E. Modulation of NMDA receptor activity in fibromyalgia. *Biomedicines* **2017**, 5 (2), 15.
30. Browne, L. E.; Blaney, F. E.; Yusaf, S. P.; Clare, J. J.; Wray, D. Structural determinants of drugs acting on the Nav1.8 channel. *J. Biol. Chem.* **2009**, 284 (16), 10523–10536.
31. Wang, M.; Li, W.; Wang, Y.; Song, Y.; Wang, J.; Cheng, M. In silico insight into voltage-gated sodium channel 1.7 inhibition for anti-pain drug discovery. *J. Molecul. Graph. Model.* **2018**, 84, 18–28.
32. Hernandez, C. C.; Tarfa, R. A.; Limcaoco, J. M. I.; Liu, R.; Mondal, P.; Hill, C.; Duncan, R. K.; Tzounopoulos, T.; Stephenson, C. R.; O'Meara, M. J.; Wipf, P. Development of an automated screen for Kv7. 2 potassium channels and discovery of a new agonist chemotype. *Bioorgan. Med. Chem. Lett.* **2022**, 71, 128841.
33. El fadili, M.; Er-raji, M.; Imtara, H.; Kara, M.; Zarougui, S.; Altwaijry, N.; Al kamaly, O.; Al Sfouk, A.; Elhallaoui, M. 3D-QSAR, ADME-Tox in silico prediction and molecular docking studies for modeling the analgesic activity against neuropathic pain of novel NR2B-selective NMDA receptor antagonists. *Processes* **2022**, 10 (8), 1462.
34. Mali, S. N.; Pandey, A.; Bhandare, R. R.; Shaik, A. B. Identification of hydantoin based Decaprenylphosphoryl- β -D-Ribose Oxidase (DprE1) inhibitors as antimycobacterial agents using computational tools. *Sci. Rep.* **2022**, 12 (1), 16368.
35. Mali, S. N.; Pandey, A. Multiple QSAR and molecular modelling for identification of potent human adenovirus inhibitors. *J. Indian Chem. Soc.* **2021**, 98 (6), 100082.
36. Mali, S. N.; Sawant, S.; Chaudhari, H. K.; Mandewale, M. C. In silico appraisal, synthesis, antibacterial screening and DNA cleavage for 1, 2, 5-thiadiazole derivative. *Current Comput.-Aided Drug Des.* **2019**, 15 (5), 445–455.
37. Ghosh, S.; Mali, S. N.; Bhowmick, D. N.; Pratap, A. P. Neem oil as natural pesticide: Pseudo ternary diagram and computational study. *J. Indian Chem. Soc.* **2021**, 98 (7), 100088.
38. Mali, S. N.; Pandey, A. Synthesis of new hydrazones using a biodegradable catalyst, their biological evaluations and molecular modeling studies (Part-II). *J. Comput. Biophys. Chem.* **2022**, 21 (7), 857–882.